A high-pressure study of $PbCO_3$ by XRD and Raman spectroscopy*

ZHANG Yu-Feng(张玉峰)[1;2)] LIU Jing(刘景)[1;1)] QIN Zhen-Xing(秦振兴)[2] LIN Chuan-Long(林传龙)[1]
XIONG Lun(熊伦)[1] LI Rui(李蕊)[1] BAI Li-Gang(白利刚)[1]

[1] Institution of High Energy Physics, Chinese Academy of Sciences, Beijing 100049, China
[2] Department of Physics, South China University of Technology, Guangzhou 510640, China

Abstract: The pressure-induced phase transitions of $PbCO_3$ are studied using synchrotron radiation in a diamond anvil cell at room temperature. The XRD measurement indicates that $PbCO_3$ with an initial phase of aragonite-type structure undergoes two phase transitions at ∼7.8 GPa and ∼15.7 GPa, respectively. The higher-pressure phase appearing at ∼15.7 GPa is stable up to 51.8 GPa. The two phase transitions are further confirmed by Raman scattering up to 23.3 GPa. During the decompression process, the high-pressure phases of $PbCO_3$ are gradually recovered to the starting aragonite-type structure, but exhibit some hysteresis. The bulk modulus B_0 of the aragonite-type structure is obtained to be 63±(3) GPa by fitting the volume-pressure data to the Birch–Murnaghan equation of states with B_0' fixed to 4.

Key words: XRD, Raman, phase transition, bulk modulus

PACS: 62.50.-p, 64.60.A-, 64.30.Jk **DOI:** 10.1088/1674-1137/37/3/038001

1 Introduction

$PbCO_3$ has been widely studied because of its technological and industrial applications. For example, $PbCO_3$ is a candidate material used for a high density and high rate gamma ray radiation detectors [1]. It could be also used as positive paste material for lead acid batteries [2] and combustion catalysts [3]. In addition, as one of the most abundant carbonate minerals in the Earth/s mantle, $PbCO_3$ plays an important part in its carbon cycle. Therefore, it is important to explore the physical behaviors, especially the phase transitions, of $PbCO_3$ under high pressure.

Under ambient conditions, $PbCO_3$ has an aragonite-type structure with a space group of Pmcn and Z=4 [4–6], which is called the $PbCO_3$- I phase. The pressure-induced phase transitions of $PbCO_3$ were studied by Raman and IR spectroscopy. However, the previous results are still controversial. For example, Lin et al. observed a phase transition starting at ∼17 GPa and completed at ∼21 GPa by using Raman spectroscopy [7]. This new phase was also observed below 4 GPa and at 1000 ℃ by using X-ray diffraction and was confirmed to have an orthorhombic structure with a space group of $P2_122$ and Z=16 [8]. On the other hand, Catalli et al. studied the $PbCO_3$ by using IR spectroscopy up to 41 GPa. However, they observed only a trigonal structure with space group P−31c and Z=2 [9] at ∼15 GPa. More recently, two pressure-induced phase transitions were observed, respectively, at ∼8 and ∼16 GPa by Minch [10]. This phase transition occurring at 8 GPa was never observed in earlier studies. In order to confirm the above phase transitions, high-pressure X-ray diffraction and Raman spectra are used to observe the phase transitions of $PbCO_3$ up to 51.8 GPa and 23.3 GPa, respectively, in this paper.

2 Experiments

A commercially available $PbCO_3$ sample (purity of 99.999%) was purchased from Alfa Aesar. The structure of the sample was confirmed by X-ray diffraction under ambient conditions and only a single phase of aragonite-type was found. In our high-pressure X-ray diffraction experiment, $PbCO_3$ powder with a ruby chip was loaded into a 100-μm-diameter hole which was drilled through the center of a pre-indented 35-μm-thick T-301 stainless steel gasket. Silicone oil was used as a pressure-transmitting medium. The sample pressure was calibrated by the frequency shift of the ruby R_1 luminescence line [11]. In situ angle dispersive X-ray diffraction (ADXD) experiments under high pressure were carried

Received 18 April 2012, Revised 7 June 2012

∗ Supported by Chinese Academy of Sciences (KJCX2-SW-N20, KJCX2-SW-N03) and National Basic Research Program of China (2011CB808200)

1) E-mail: liuj@ihep.ac.cn

2) E-mail: yfzhang@ihep.ac.cn

out at the 4W2 Beamline of the Beijing Synchrotron Radiation Facility (BSRF) with a wavelength of 0.6199 Å. The X-ray diffraction patterns were collected by an image plate detector (MAR345) and the two-dimensional diffraction patterns were integrated using the program FIT2D to yield one-dimensional plots of X-ray intensity as a function of d-spacing [12].

The Raman spectra were measured in a backscattering configuration by using a confocal Raman spectrometry system. The 488 nm Ar^+ laser line was used for excitation with a focused beam of 2–3 μm in diameter on the samples. Raman signals were dispersed by a Spectrapro 500i spectrograph equipped with a 1800 gr/mm grating and detected by using a liquid-cooled charge-coupled-device (CCD) camera. The Raman frequency calibration was carried out by using a standard Ne lamp with known line-spectral peak frequencies. In the Raman spectra, the positions of the Raman peaks were fitted by using a Lorentzian profile.

3 Results and discussion

Figure 1 shows the typical X-ray diffraction patterns of $PbCO_3$ under high pressure. The X-ray diffraction pattern at 3.1 GPa can be indexed as an aragonite-type structure and is labeled as the $PbCO_3$-Ⅰ phase, as shown in Fig. 1(a). With pressure increasing, the X-ray diffraction peaks shift to higher angles and become broader, which leads to the overlapping of some peaks. However, no new diffraction peak appears on the X-ray diffraction patterns up to 7.8 GPa, indicating that $PbCO_3$ keeps the aragonite-type structure below ∼7.8 GPa. At about 7.8 GPa, a new peak (marked with an arrow) appears at 2θ of 7.6° (d=4.68Å), suggesting the onset of a phase transition of $PbCO_3$. The new phase appearing at 7.8 GPa is in agreement with Minch's results, but was not observed by Lin and Catalli et al. This new phase is labeled as the $PbCO_3$-Ⅱ phase but we fail to solve its structure due to the lack of enough new peaks. Above 7.8 GPa, the diffraction peaks of the $PbCO_3$-Ⅰ phase still exist but their relative intensities become weaker. $PbCO_3$-Ⅰ and $PbCO_3$-Ⅱ phases coexist in the pressure range of 7.8–15.7 GPa. Above 15.7 GPa, five new peaks can be observed at 2θ of 9.7, 12.5, 12.8, 13.7 and 16.9°, respectively, as marked by the arrows in Fig. 1(c). However, the five new peaks can not be reasonably indexed. With the pressure increasing, these new peaks become stronger, which implies that $PbCO_3$ undergoes another phase transition at 15.7 GPa. This new phase was also reported in earlier studies and is labeled the $PbCO_3$-Ⅲ phase here. Upon compression to 21.7 GPa, another peak (marked with an arrow) appears at 2θ of 7.8° (d=4.56Å) as shown in Fig. 1(b). This new peak can be attributed to the $PbCO_3$-Ⅲ phase according to Liu's point of view [7]. But the first new peak appearing at 7.8 GPa disappears as the pressure reaches 21.7 GPa, which means that the $PbCO_3$-Ⅱ phase disappears. With the pressure further increasing to the highest pressure (51.8 GPa), there is no observable new phase except for the peak-position shifts of the existent phase.

The pressure dependence of the d-spacing is shown in Fig. 2. It can be found that the new and discontinuous d-spacings occur at ∼7.8 GPa (Fig. 2(b)) and ∼15.7 GPa (Fig. 2(c)), respectively. This indicates that the $PbCO_3$ indeed undergoes phase transitions in these pressure ranges.

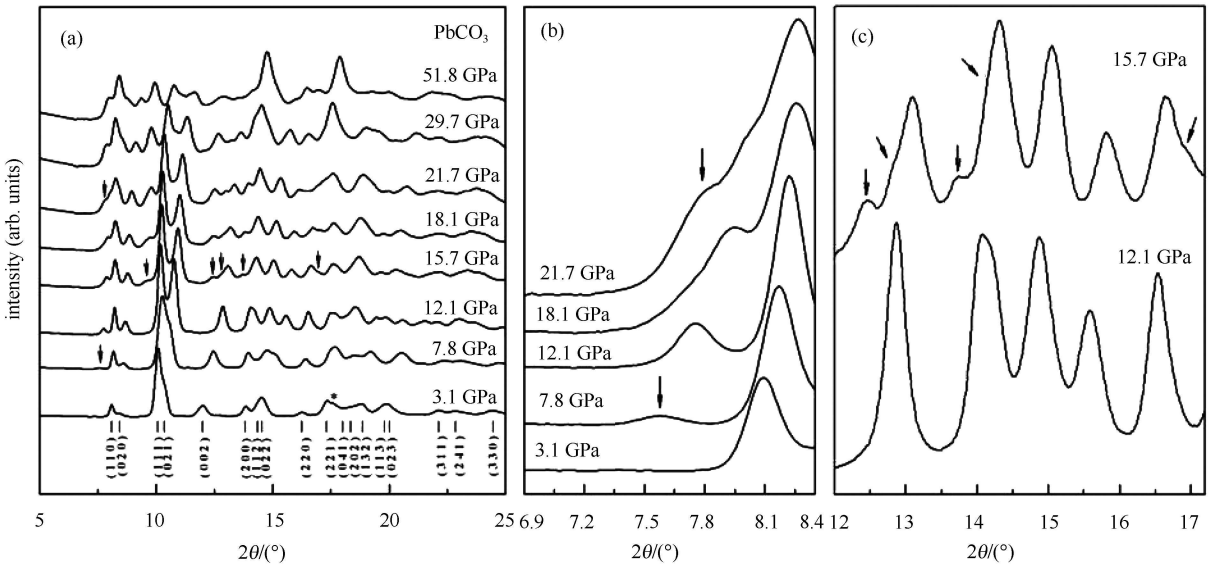

Fig. 1. (a) Representative XRD patterns of $PbCO_3$ at different pressures, the peak marked with ∗ at 3.1 GPa is from gasket; (b) enlarged patterns in the angle range of 6.9°–8.4°; (c) enlarged patterns in the angle range of 12°–17°.

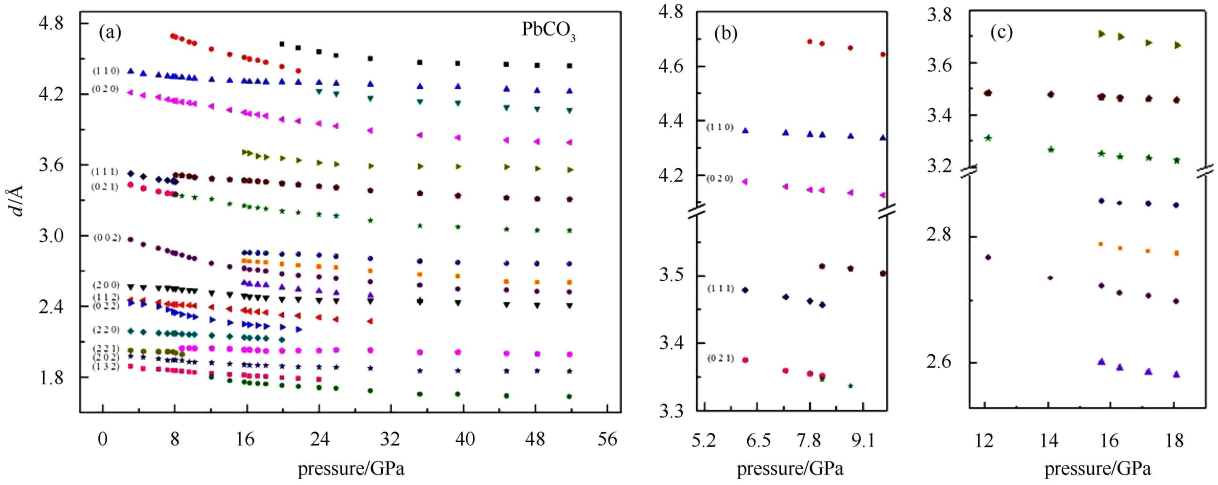

Fig. 2. (a) The pressure dependence of d-spacing; (b) The enlarged patterns in the pressure range of 5.2–9.1 GPa; and (c) The enlarged patterns in the pressure range of 12–18 GPa.

The diffraction patterns during the decompression process are shown in Fig. 3. When the pressure is decompressed to 0.3 GPa, the pattern can be well indexed as the $PbCO_3$- Ⅰ phase, for except a faint peak marked by the arrow belonging to the high-pressure structure.

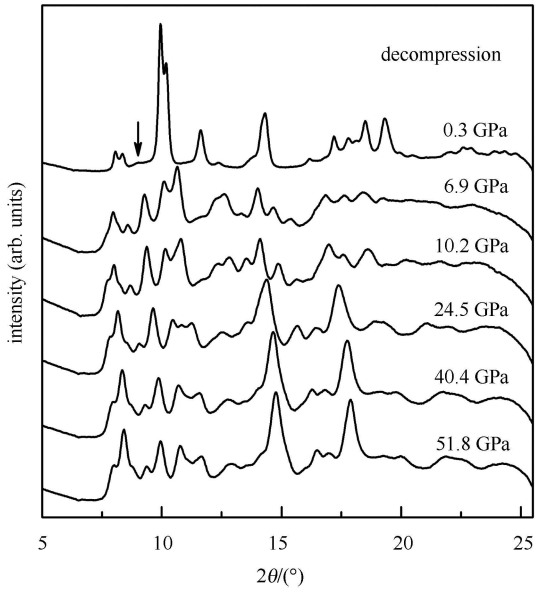

Fig. 3. Angle-dispersive XRD patterns of $PbCO_3$ for decompression.

The structure was refined by using the GASA+EXPGUI program based on the Le-Bail method [13] for this pattern and the result is shown in Fig. 4. The lattice parameters obtained by the structural refinement for the quenched phase are a=5.147(5) Å, b=8.501(2) Å and c=6.120(3) Å, which agrees well with the aragonite-structure [4]. It suggests that the phase transition is reversible and the high-pressure $PbCO_3$- Ⅱ and $PbCO_3$- Ⅲ are kinetically unstable under ambient conditions.

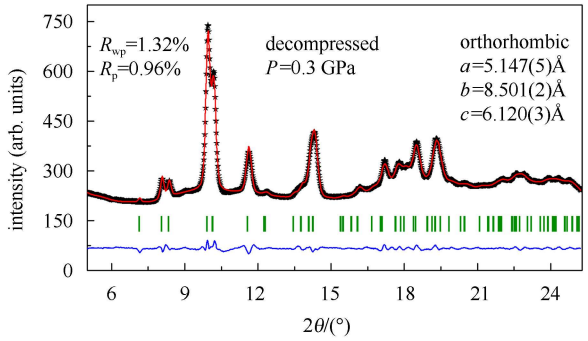

Fig. 4. Le Bail refinement of the XRD pattern of $PbCO_3$ at pressure of 0.3 GPa after decompression. The symbols, the upper solid line, and the lower solid line represent the observed and calculated patterns and their differences, respectively. The rows of vertical bars indicate the expected positions of diffraction peaks.

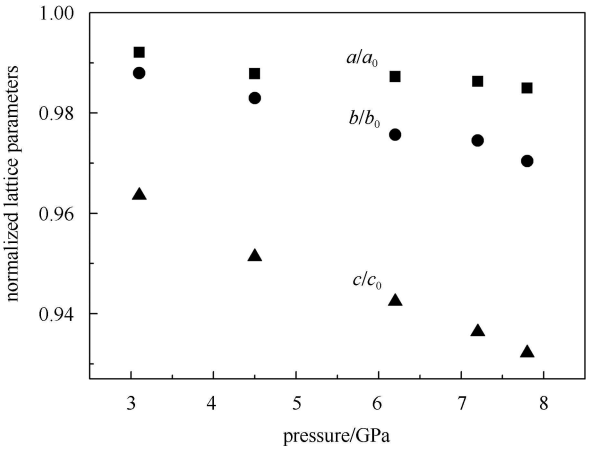

Fig. 5. Compressibility of the normalized lattice parameters of the $PbCO_3$- Ⅰ phase.

Figure 5 shows the pressure dependence of the normalized lattice parameters of the $PbCO_3$- Ⅰ phase. The relative changes along the a-axis, b-axis and c-axis are 0.72(3)%, 1.78(3)% and 3.26(4)%, respectively. Obviously, it is more compressible along the c-axis.

The pressure dependence of the unit-cell volume for the $PbCO_3$- Ⅰ phase is shown in Fig. 6. The P–V data are fitted to the third-order Birch-Murnaghan equation of the state [14],

$$P(V) = \frac{3B_0}{2}\left[\left(\frac{V_0}{V}\right)^{7/3} - \left(\frac{V_0}{V}\right)^{5/3}\right] \cdot \left\{1+\frac{3}{4}(B_0'-4)\left[\left(\frac{V_0}{V}\right)^{2/3}-1\right]\right\},$$

where B_0 is the bulk modulus at ambient pressure, B_0' is the pressure derivative of B_0, and V_0 is the volume at ambient pressure. The least-squares fitting yields values of B_0=63 (3) GPa and V_0=67.1(2) Å^3 with B_0' fixed at 4.

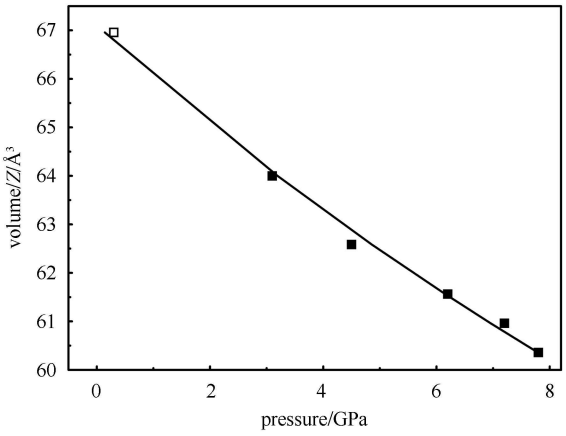

Fig. 6. The pressure dependence of the unit cell of every formula for the $PbCO_3$- Ⅰ phase. The compression curve is obtained by fitting the data to the third-order Brich-Murnaghan equation of state. The solid and hollow squares show the data from compression and decompression, respectively.

In order to confirm the phase transitions observed in the X-ray diffraction, the Raman experiment was performed under high pressure. As shown in Fig. 7(a), parts of Raman peaks in the range of 600–1600 cm^{-1} are clearly observed. In Fig. 7(b), different numbers denote different Raman peaks with assignments labeled on the left or right side. The new peaks are shown by the arrows. The initial Raman spectrum was measured at 2.4 GPa. All the observed frequencies in this study have been well assigned and agree well with the previous studies [10, 15, 16]. At about 7.0 GPa, the B_{3g} mode (in-plane band of CO_3^{2-} groups) at 671 cm^{-1} and the A_{1g} mode (in-plane band of CO_3^{2-} groups) at 675 cm^{-1} coalesce into a broad peak. Some new peaks which appear at 10.4 GPa are indicated by arrows in Fig. 7(a). According to the previous study [10], the new peaks indicate the formation of the $PbCO_3$- Ⅱ phase. The transformation pressure from $PbCO_3$- Ⅰ to $PbCO_3$- Ⅱ is slightly higher than that in the X-ray diffraction. This difference could be due to different hydrostatic environments in the two experiments. Another possible reason is that the new Raman peak is too weak to be observed below 10.4 GPa.

At the pressure of 15.9 GPa, another new peak appears at 840 cm^{-1}, indicating a phase transition from $PbCO_3$- Ⅱ to $PbCO_3$-Ⅲ. These results agree with those obtained from the X-ray diffraction.

As shown in Fig. 7(b), the A_{1g} mode at 839.2 cm^{-1} exhibits softening behavior. It has a negative linear shift of −1.64(9) cm^{-1}/GPa. The negative shift usually appears in carbonate minerals [4, 10] and is caused by the out-of-plane bending vibrations. In addition, the X-ray diffraction (Fig. 5) demonstrates that there is an enhanced compressibility along the c-axis with increasing pressure. Therefore, we think that the interaction between the oxygen anions and carbons in the neighboring layers is strengthened.

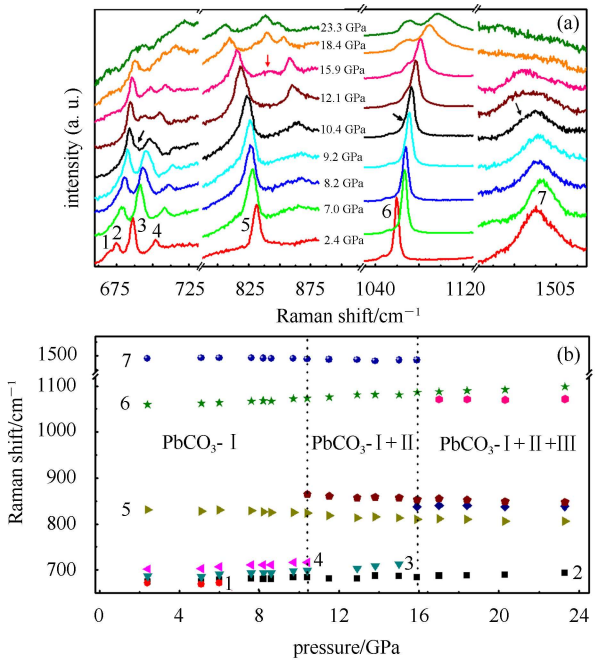

Fig. 7. (a) The representative Raman spectra of $PbCO_3$ at different pressures in the 600–1600 cm^{-1} frequency regions; (b) Pressure-induced mode shifts of the out-of-plane (ν_2) and in-plane (ν_4) bending of CO_3^{2-} groups: 1 B_{3g} (ν_4-in-plane), 2 A_{1g} (ν_4-in-plane), 3 B_{2g} (ν_4-in-plane), 4 B_{1g} (ν_4-in-plane), 5 A_{1g} (ν_2-out-of-plane), 6 A_{1g} (ν_1-symmetric C-O stretching of CO_3^{2-} groups), 7 (ν_3-symmetric C-O stretching of CO_3^{2-} groups).

4 Conclusion

The X-ray diffraction experiment shows that the aragonite-type $PbCO_3$ ($PbCO_3$- Ⅰ) could undergo two phase transitions. The transformation from $PbCO_3$- Ⅰ to $PbCO_3$-II and to $PbCO_3$-Ⅲ occurs at ∼7.8 GPa and ∼15.7 GPa, respectively. The high-pressure phases of $PbCO_3$ are recovered to the $PbCO_3$- Ⅰ phase when the pressure is released. These results are in good agreement with Minch's Raman measurements. Two phase transitions are also observed at 10.4 GPa and 15.9 GPa in Raman spectroscopy.

The bulk moduli and its first pressure derivative of $PbCO_3$- Ⅰ phase are obtained by fitting the P-V data to the third-order Birch-Murnaghan equation of state: B_o=63±(3) GPa when fixed B_0'= 4. The negative shift of the ν_2–out-of-plane band of CO_3^{2-} groups is related to the largest compression along the c-axis.

This work was performed at the 4W2 Beamline at the BSRF.

References

1 Moses W W et al. IEEE Transactions on Nuclear Science, 1991, **38**: 648–653
2 BAO Y F et al. Battery Bimonthly, 2002, **32**: 230–232
3 Bakhman N N et al. Combustion and Flame, 1971, **17**: 383–389
4 Speer J A et al. Carbonates: Mineralgoy and Chemistry. Washington D C, 1983. 145–190
5 Chevrier G et al. Zeitschrift fur Kristallographie, 1992, **199**: 67–74
6 Sytle M ANTAO et al. the Canadian Mineralogist, 2009, **47**: 1245–1255
7 LIN C C et al. J. Phys. Chem. Sol., 1997b, **58**: 977–987
8 LIN C C et al. Phys. Chem. Miner., 1997a, **24**: 149–157
9 Catalli K, Santillian J et al. Phys. Chem. Miner., 2005, **32**: 412–417
10 Robert Minch et al. Phys. Chem. Miner., 2010, **37**: 45–56
11 MAO H K, XU J, Bell P M et al. J. Geophys. Res., 1986, **91**: 4673–4676
12 Hammersley A P et al. High Press Res., 1996, **14**: 235–248
13 Larson A C, Von Dreele R B. General Structure Analysis System, Los Alamos National Laboratory Report LAUR, 2004. 86–748
14 Aderson O L. Equation of State of Solids for Geophysics and Ceramic Science. New York: Oxford University, 1995.
15 Herman R G, Bogdan C E et al. Appl. Spectrosc., 1987, **41**: 437–440
16 Coleyshaw E E, Griffith W P et al. Spectrochimica Acta, 1994, **50A**: 1909–1918